

A Single-Phase Grid-Connected PV System With Active Power Filter

Denizar C. Martins and Kleber C. A. de Souza

Abstract—In this paper a single-phase active power filter based in a two stages grid-connected photovoltaic system is presented. The proposed system can not only inject PV power into utility but can act always as an active power filter to compensate the load harmonics and reactive power such that the input power factor is unity independently of the solar radiation. In sunny days, the system processes all the reactive and active load power and the excessive power from the PV module can be fed to the utility. On the other hand, on cloudy days for instance, if the PV power is not enough, the system processes all the reactive load power and the shortage of load active power is supplemented by the utility. Besides, just using one current sensor, the control strategy is simpler and of easy practical implementation.

Keywords—Active power filter, grid-connected, power factor, PV systems, single-phase systems, THD.

I. INTRODUCTION

PHOTOVOLTAIC (PV) solar energy as an alternative resource has been becoming feasible due to enormous researches and development work being conducted over a wide area (Bahu, 1996), (Chiang, 1998), (Hirachi, 1996) and (Yamaguchi, 1994).

Some researchers spent efforts in developing PV inverter systems with grid connection and active power filtering features using sensors to measure the load current (Wu, 2005), (Kim, 1996), (Cheng, 1997) and (Kuo, 2001).

This paper presents a single-phase topology, without load current sensor, composed by a dc-dc converter in cascaded with an inverter, as shown in Fig. 1. The system aims transferring the photovoltaic (PV) power to the ac load and paralleled with the utility. The dc-dc converter is used to boost the PV voltage to a level higher than the peak of the voltage utility such that the inverter can provide the ac voltage without requiring the transformer. The dc-dc converter is also responsible for tracking the maximum power point (Koutroulis, 2001) and (Zhang, 200) of the PV modules to fully utilize the PV power. The shortage of load power from the PV module is supplemented by the utility. On the contrary, the excessive power from the PV module to the load can be

D. C. Martins is with the Power Electronics Institute (INEP) at Federal University of Santa Catarina, Florianopolis, SC, Brazil (corresponding author to provide phone: +55-48-3721-9204; fax: +55-48-3234-5422; e-mail: denizar@inep.ufsc.br).

K. C. de Souza is with the Power Electronics Institute (INEP) at Federal University of Santa Catarina, Florianopolis, SC, Brazil (phone: +55-48-3721-9204; fax: +55-48-3234-5422; e-mail: ksouza@inep.ufsc.br). Manuscript received May 3, 2008; Revised received June 22, 2008

fed to the utility. The balance of power flow is controlled through the inverter. The inverter also is used to act always as an active power filter to compensate the load harmonics and reactive power such that the input power factor is unity (Fig. 2).

II. PROCEDURE FOR PAPER SUBMISSION

The dc-dc converter power structure used to boost the PV voltage and for tracking the maximum power point of the PV modules to fully utilize the PV power was the Half-Bridge Zero Voltage Switching Pulse Width Modulation (DC-DC HB ZVS-PWM) asymmetrically driven converter (de Souza, 2006) shown in Fig.3.

The HB ZVS-PWM has been designed considering the reduction of losses and mainly the volume of the magnetic and the right value of the capacitors $Ce1$ and $Ce2$ can be determined by (1) and (2).

$$Ce_1 = \frac{P_o}{f_s \cdot \Delta V_{C_{eq}} \cdot V_i} \cdot (1-D) \quad (1)$$

$$Ce_2 = \frac{P_o}{f_s \cdot \Delta V_{C_{eq}} \cdot V_i} \cdot D \quad (2)$$

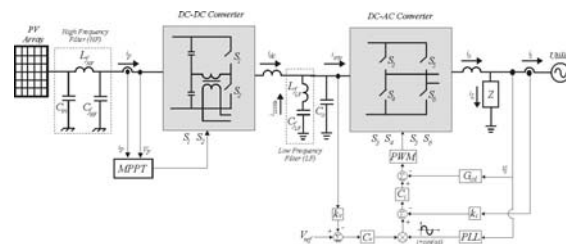


Fig. 1 Single-phase two stages Active Power System PV system.

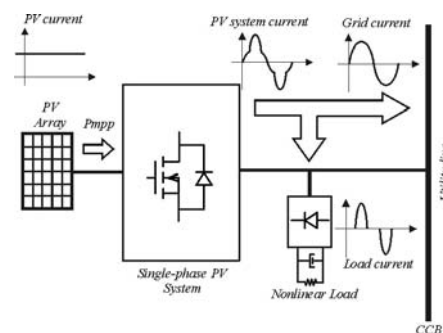


Fig. 2 Power flow of the system with nonlinear load.

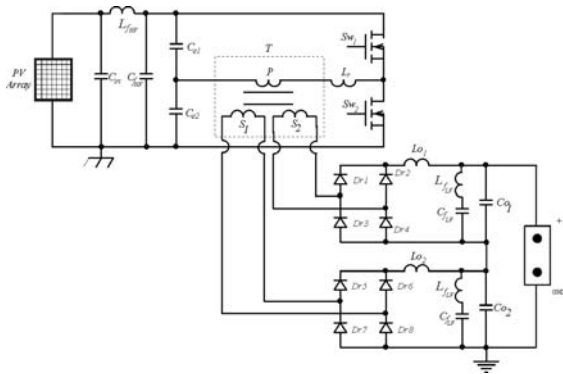


Fig.3 Half-Bridge Zero Voltage Switching.

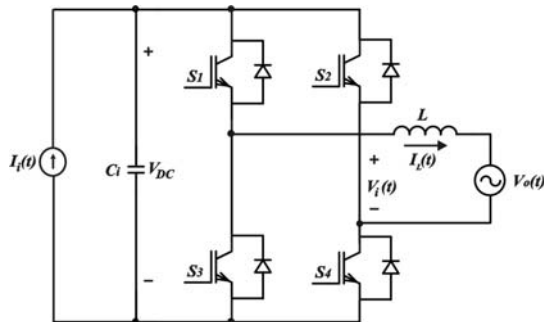


Fig. 4 Full bridge inverter.

Fig. 4 presents the full bridge topology with the inductor L connected between the grid ($V_o(t)$) and the inverter, the capacitor C_i in the structure input representing the DC voltage source and a current source ($I_i(t)$), that can be either the output of the DC-DC converter or an array of photovoltaic panels.

Considering the self-commutated inverter switching at high frequency and using three level PWM technique, it is possible to represent the four equivalent circuits of the switching modes (Fig. 5), defined by the combination of the switches possible states with the two possible direction of the output current.

From the operational stages, it can be observed that when $I_L(t) > 0$ and the switches S_1 e S_4 are on, voltage $V_i(t)$ has its polarity defined by the direction of the output current, with its absolute value equal to input voltage V_{DC} , whose amplitude should be larger than the peak value of the output voltage, $V_o(t)$. In this manner, the voltage polarity across the inductor causes its current's absolute value to increase. During this stage, energy from the input source, V_{DC} , along with part of the energy stored in the inductor, is transferred to the grid. When $I_L(t) > 0$ and the switches S_2 and S_3 are on, voltage $V_i(t)$ is zero. In this manner, the voltage polarity across the inductor is inverted, causing its current's absolute value to decrease. Indeed, the output current is controlled by imposing the derivative of the current through the inductor, or, put differently, by imposing the voltage across the inductor L . In this manner, the structure of the converter shown in Fig. 4 can be represented, without loss of generality, as the controlled voltage source $V_i(t)$, presented in Fig. 6 where the link

inductors are represented by the inductor L , $V_o(t)$ is the utility voltage and $I_L(t)$ is the output PV system current.

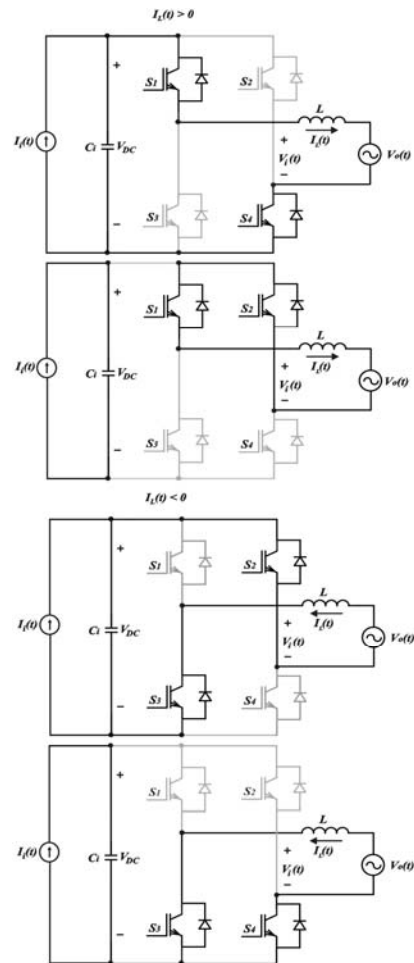


Fig. 5 Four equivalent circuits of the switching modes.

In Fig. 6 the energy flow is controlled by the current $I_L(t)$. However, this current is defined by the difference of voltage between the sources $V_i(t)$ and $V_o(t)$, applied across the impedance. In this case, as the impedance is a pure inductance, the current will be equal the integral of the voltage across it. As $V_o(t)$ is known, once it is the utility voltage itself, $V_i(t)$ is imposed and therefore $V_L(t)$, in a convenient form, in a way to obtain the output current desired across the inductor. Thus:

$$V_L(t) = V_i(t) - V_o(t) \quad (3)$$

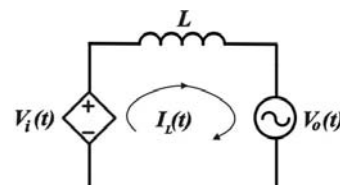


Fig. 6 Simplified equivalent inverter circuit.

PWM defines a modulated signal composed of the reproduction of the modulating signal's spectrum, whose

amplitude is defined by the modulation, added to harmonic components of frequencies that are multiples of the switching frequency. Ignoring the effect of the harmonic components of the switching frequency on voltage $V_i(t)$, once the inductor works as a low pass filter for the current, the voltage imposed across the inductor is represented simply by (3). Fig. 7 shows the manner in which the converter allows the voltage to be imposed across the inductor, as shown in the equivalent circuit of Fig. 6.

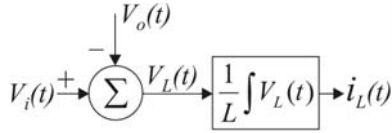


Fig. 7 Block diagram of the simplified equivalent circuit.

Indeed, the output current is desired to be a mirror of $V_o(t)$ as expressed in (4). Nevertheless, according to (5), the inductor voltage is the derivative of the current across itself. Therefore, equation (6) describes the voltage $V_i(t)$, which, in effect, is defined by the control loop, should present a sine, in order to annul the effect of $V_o(t)$, and a cosine, which, by composition, will be the resulting voltage imposed across the inductor, therefore, guaranteeing a sinusoidal current. In practice, at the frequency of the grid, the inductor is a very small reactance, causing the voltage drop across the inductor to be smaller than the utility voltage. In other words, the sine of $V_i(t)$ dominates the cosine, demonstrating that the demand on the current loop is much more in favor of annulling the "disturbance" of the utility voltage rather than to effectively control the output current.

$$I_L(t) = I \cdot \sqrt{2} \cdot \sin(\omega t) \quad (4)$$

$$V_L(t) = L \cdot \frac{dI_L(t)}{dt} = L \cdot I \cdot \sqrt{2} \cdot \omega \cdot \cos(\omega t) \quad (5)$$

$$V_i(t) = L \cdot I_{rms} \cdot \sqrt{2} \cdot \omega \cdot \cos(\omega t) + V_{rms} \cdot \sqrt{2} \cdot \sin(\omega t) \quad (6)$$

In the classic control strategy, an internal current loop and an external loop to control the input voltage are implemented. The voltage loop defines the amplitude of the reference current by multiplying its control signal by a "waveform", which can be a sample of the output voltage or a digitally generated sinusoid, generating the output current reference. Fig. 8 demonstrates how the classic control strategy is implemented, in which $V_i(t)$ is determined by the current error signal passing through the compensator and the error signal is the difference between a sample of the current and its reference. Fig. 9 shows the same block diagram simplified.

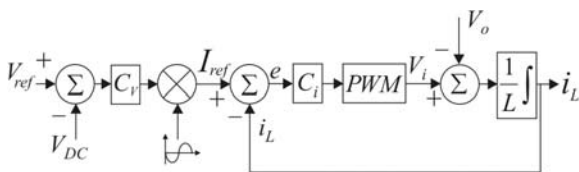


Fig. 8 Block diagram of classical control strategy current loop.

It is observed, however, that the output voltage $V_o(t)$

appears as a disturbance in the simplified traditional model. Therefore, voltage $V_i(t)$, which, in effect, is defined by the control loop should present a sine, in order to annul the effect of $V_o(t)$, and a cosine, which, by composition, will be the resulting voltage imposed across the inductor, therefore, guaranteeing a sinusoidal current. In practice, at the frequency of the mains, the inductor is a very small reactance, causing the voltage drop across the inductor to be much smaller than the voltage of the mains. In other words, the sine of $V_i(t)$ dominates the cosine, demonstrating that the demand on the current loop is much more in favor of annulling the "disturbance" of the output voltage rather than to effectively control the output current.

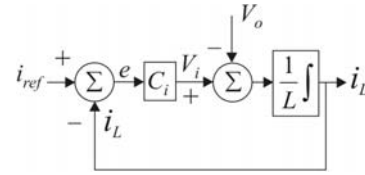


Fig. 9 Simplified block diagram of classical control strategy current loop.

Rewriting equation (3) as in (7) (Kuo, 2001):

$$L \cdot \frac{di_L(t)}{dt} = k \cdot v_{control}(t) - V_o(t) \quad (7)$$

$$k = \frac{V_{DC}}{V_{tri}} \quad (8)$$

Where V_{tri} is the peak of the triangular carrier signal and $v_{control}$ is the control signal which shapes the sinusoidal current to the utility line. From the block diagram, the current signal error is equal (9).

$$e(t) = i_{Lref}(t) - i_L(t) \quad (9)$$

Sense a perfect sinusoidal current to the utility line is a designed goal, e must naturally approach zero. Thus, deriving (9) and substituting (7) into (10):

$$\frac{de(t)}{dt} = 0 = \frac{di_{Lref}(t)}{dt} - \frac{di_L(t)}{dt} \quad (10)$$

$$v_{control}(t) = \frac{L}{k} \cdot \frac{di_{Lref}(t)}{dt} + \frac{1}{k} \cdot V_o(t) \quad (11)$$

As the disturbance is measurable, the utility voltage disturbance controller G_{cd} is used to reduce the disturbed voltage component. The new block diagram that contains this feed-forward controller is presented in Fig.10. From Fig.10, it can be seen that:

$$i_L = \frac{k \cdot C_i}{sL + k \cdot C_i} \cdot I_{Lref} + \frac{k \cdot (G_{cd} - 1/k)}{sL + k \cdot C_i} \cdot V_o \quad (12)$$

From (12), when $G_{cd} = 1/k$, the disturbance from V_o can be eliminated, and if $kC_i \gg |sL|$, then $I_L = I_{ref}$, identifying accurate current control effect for I_{ref} .

Repeating the same analysis, but now considering the connection of any load between the system and the commercial electric grid, a new configuration, presented in

Fig. 11, is obtained. It can be observed that now the inductor current is the load current plus the utility current. Again, as sinusoidal current to the utility line is a designed goal, adding a sample of the load current to the inductor current reference it is possible to control the inductor current and still guarantee a sinusoidal utility current. A new block diagram representing the system is shown in Fig. 11.

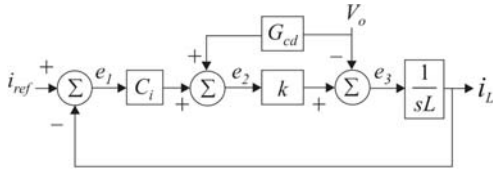


Fig.10 Block diagram containing the feed-forward controller.

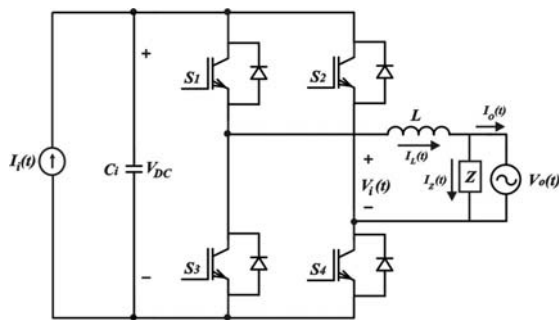


Fig. 11 PV system with any load connected.

However, in this case, besides the current sensor used to sample the current in L , it is necessary another sensor to sample the current in the load. Another disadvantage in this configuration is that as the control is done monitoring the load current (I_z), when the system is operating Active Power Line Conditioner Mode (low sun light), is necessary before to extract the fundamental component of the load current for later to find the reference current. So, it is necessary to observe a period of the grid at least.

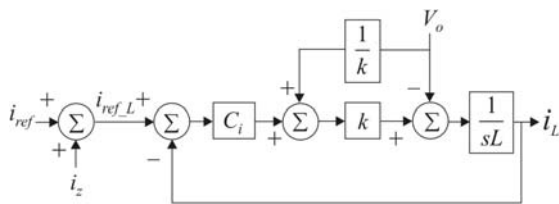


Fig. 12 New block diagram of the inductor current loop.

However, sensing the AC mains current instead of the inductor current, and considering that the difference between the inductor current and the load current is the utility current, the last block diagram can be modified to represent now the utility current loop (Fig. 13). Nevertheless, according to Fig. 8, $i_{o_ref}(t)$, or, the difference between the reference inductor current (i_{L_ref}) and the load current (I_z), is exactly the own i_{ref} defined by the voltage control signal multiplied by a sinusoid in phase with the utility frequency (Fig. 14). Thus, the same system can be controlled observing only the utility current directly (I_o), improving the dynamics of the system, once it

will be not necessary any previous calculation.

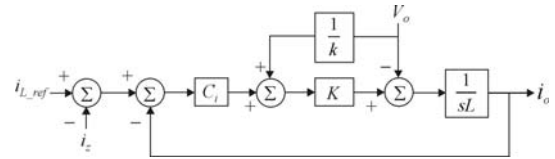


Fig. 13 Block diagram of the utility current loop.

Thus, to control the output current in phase with the voltage utility and, to obtain a unity power factor, even with the connection of a load between the grid and the system, it is enough to observe only the AC mains current. In this case, besides doing use of just a sensor one, the control strategy is simpler and of easy practical implementation.

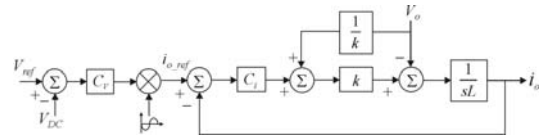


Fig. 14 Utility current control diagram.

III. EXPERIMENTAL RESULTS

To demonstrate the feasibility of the discussed PV system, a prototype was designed and implemented. The specifications of the system (Figure 15 and Figure 16) are shown below.

Solar array:

- Number of PV Module: 20;
- Rated power: 1002W;
- Rated voltage: 83.5V;
- Rated current: 12A;
- Short-circuit current: 12.4A;
- Open-circuit voltage: 107V.

Dc-dc power converter:

- Output voltage: 400V;
- Switching frequency: 100kHz;
- C_{in} and C_{fHF} : 1000 μ F;
- C_{e1} and C_{e2} : 10 μ F and 5 μ F;
- L_{fHF} and L_r : 50 μ H and 680nH;
- C_o : 1000 μ F.

Inverter:

- Switching frequency: 20kHz;
- C_{fLF} : 1000 μ F;
- L_{fLF} : 1.6mH;
- L_{o1} and L_{o2} : 1.2mH;
- Output voltage: 220V, 60Hz;
- Load: 400VA (Capacitivy).

In the proposed system, a LC filter (L_{fHF} and C_{fHF}) is connected with the PV array output to filter the high frequencies drained by the dc-dc converter, and a series LC filter (L_{fLF} and C_{fLF}) is connected between the converters to support the second-order component (120Hz) presented in the input inverter current.

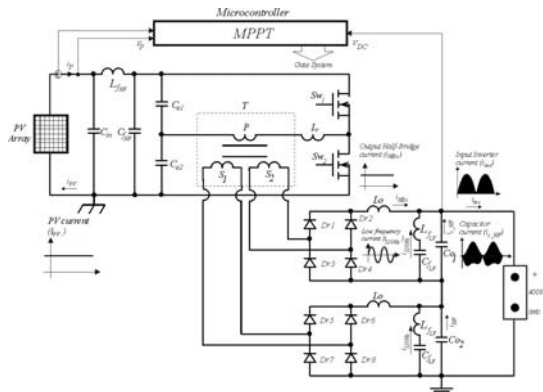


Fig. 15 Half-Bridge Zero Voltage Switching block diagram.

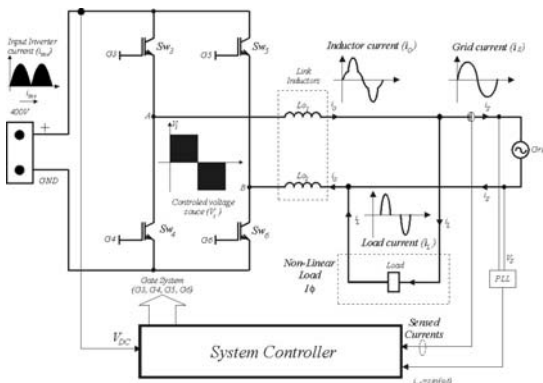


Fig. 16 Simplified block diagram of the Inverter.

Figure 17 and Figure 18 depicts, respectively, the load current (I_L), the inverter current (I_o), the voltage current ($V_{Utility}$) and utility current (I_S) with the system operating just as active power line conditioning mode (cloudy day or night). The THD of I_S is 4.0% for a load crest factor of 3.09.

Fig. 19 depicts the output inverter current (I_o) and the utility current (I_S) with the system supplying power to the load and supplying surplus power to the utility line. Fig. 20 shows the utility voltage and the utility current with the system only supplying power to the utility (THD = 2.5%).

IV. CONCLUSION

This paper presents a single-phase topology for transferring the photovoltaic (PV) power to the ac load and paralleled with the utility. The proposed PV system has the advantage of act always as an active power filter to compensate the load harmonics and reactive power such that the input power factor is unity.

The simplicity in the strategy of the output current control, in other words, current injected in the electric system, is another advantage of the study, because besides doing use of just one current sensor, it is of easy practical implementation

ACKNOWLEDGMENT

The authors would like to thank the Brazilian agencies CNPq for financial support

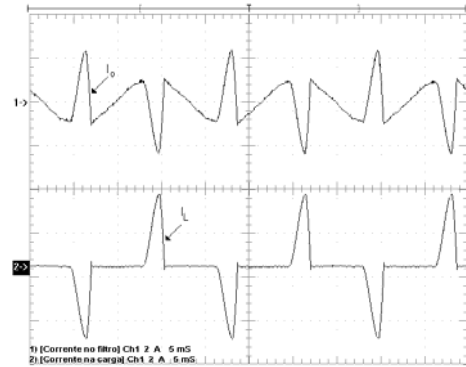


Figure 17. Waveforms of Load current (I_L) and Inverter current (I_o) (Ch1 2A/div and Ch2 2A/div).

REFERENCES

- [1] S. S. Bahu, S. Palanichamy (1996). "PC based controller for utility interconnected photovoltaic power conversion system"; *Proc. IEEE Power Electronics Specialists Conf.*, vol. 1, Jan., pp. 101–106.
- [2] L. Cheng, R. Cheung, K. H. Leung(1997). "Advanced photovoltaic inverter with additional active power line conditioning capability"; *Proc. IEEE Power Electronics Specialists Conf.*; vol. 1; pp. 279–283.
- [3] S. J. Chiang, K. T. Chang, C. Y. Yen (1998). "Residential photovoltaic energy storage system"; *IEEE Trans. Ind. Electron.*, vol. 45, no. 3, pp. 385–394.
- [4] K. C. A. de Souza, O. H. Gonçalves, D. C. Martins (2006). "Study and optimization of two dc-dc power structures used in a grid-connected photovoltaic system"; *Power Electronics Specialists Conference, PESC06*, pp. 1 – 5.
- [5] K. Hirachi, T. Mii, T. Nakashiba, K. G. D. Laknath and M. Nakaoka (1996). "Utility-Interactive multi-functional Bi-directional converter for solar photovoltaic power conditioner with energy storage batteries"; *Proc. IECON'96 Conf.*, pp. 1693–1698.
- [6] S. Kim, G. Yoo, J. Song, (1996). "A Bi-functional utility connected photovoltaic system with power factor correction and facility"; *Proc. Photovoltaic Specialists Conf.*, pp. 1363–1368.
- [7] E. Koutroulis, K. Kalaitzakis, N. C. Voulgaris (2001). "Development of a Microcontroller-Based Photovoltaic Maximum Power Point Tracking Control System"; *IEEE Transaction On Power Electronics*, v. 16, n. 1, pp. 46-54.
- [8] Y. C. Kuo, T. J. Liang, J. F. Chen, (2001). "Novel maximum-power-point tracking controller for photovoltaic energy conversion system"; *IEEE Trans. Ind. Electron.*, vol. 48, n° 3, pp. 594–601.
- [9] T. Wu, C. Shen, H. Nein, G. Li (2005). "A $1\phi/3W$ inverter with grid connection and active power filtering based on nonlinear programming and fast-zero-phase detection algorithm"; *Power Electronics, IEEE Transactions on*, Volume 20, Issue 1, Jan. 2005 pp. 218 – 226.
- [10] M. Yamaguchi, K. Kawarabayashi, T. Takuma (1994). "Development of a new utility-connected photovoltaic inverter line back"; *Proc. INTELEC'94 Conf.*, pp. 676–682.
- [11] L. Zhang, A. Al-Amoudi, Y. Bai (2000). "Real-Time Maximum Power Point Tracking for Grid-Connected Photovoltaic Generators"; *IEE Power Electronics and Variable Speed Drives Conference – PESC2000*, p. 124-129.

Denizar Cruz Martins was born in São Paulo, SP, Brazil, on April 24, 1955. He received the B.S. and M.S. degrees in electrical engineering from Federal University of Santa Catarina, Florianopolis, Brazil, in 1978 and 1981, respectively, and the Ph.D. degree in electrical engineering from Polytechnic National Institute of Toulouse, Toulouse, France, in 1986.

He is currently a Full Professor of the Department of Electrical Engineering in the Federal University of Santa Catarina, Florianopolis, Brazil. He research interest includes: dc-dc and dc-ac converters, soft commutation, power factor correction and renewable energy.

Prof. Martins is a member of IEEE and SOBRAEP (Power Electronics Brazilian Society) and SBA (Automatic Brazilian Society).

Kleber César Alves de Souza was born in Campina Grande, PB, Brazil, on September 19, 1975. He received the B.S. and M.S. degrees in electrical engineering from Federal University of Ceará, Fortaleza, Brazil, in 2000 and 2003.

He is currently a Ph.D. student of the INEP (Power Electronics Institute) in the Federal University of Santa Catarina, Florianopolis, Brazil. His research interest includes: dc-dc and dc-ac converters, power quality, power factor correction and renewable energy.

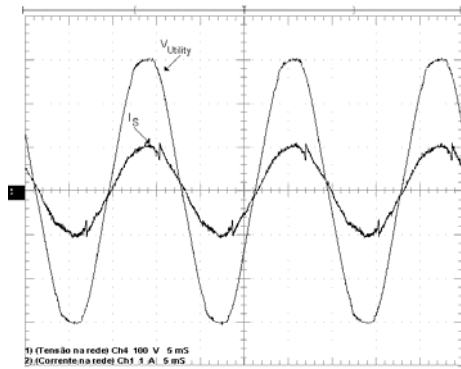


Figure 18. Utility current (I_s) and utility voltage ($V_{Utility}$) with load (Ch1 1A/div and Ch2 100V/div).

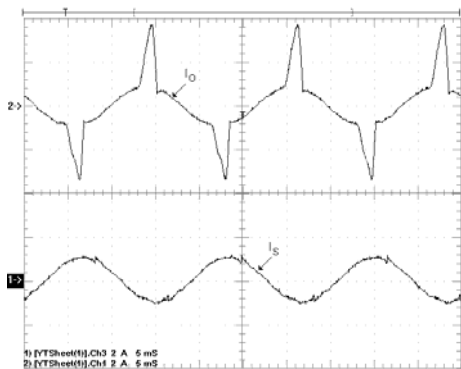


Fig. 19. Waveforms of utility current (I_s) and Inverter current (I_o) (Ch1 2A/div and Ch2 2A/div).

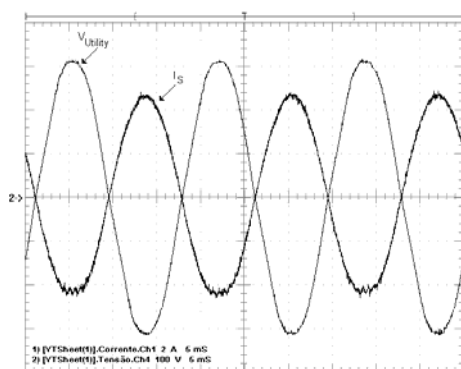


Fig. 20. Waveforms of grid current (I_s) and utility voltage ($V_{Utility}$) without load. (Ch1 2A/div and Ch2 100V/div)